ELSEVIER

International Journal of Mass Spectrometry 219 (2002) 363–371

International Journal of Mass Spectrometry

www.elsevier.com/locate/ijms

Recent gold cluster studies in a Penning trap

L. Schweikhard [a,*], K. Hansen [b], A. Herlert [c], M.D. Herráiz Lablanca [c], G. Marx [a], M. Vogel [c]

[a] Institut für Physik, Ernst-Moritz-Arndt-Universität Greifswald, D-17487 Greifswald, Germany
[b] Department of Physics, University of Jyväskylä, P.O. Box 35, FIN-40014, Jyväskylä, Finland
[c] Institut für Physik, Johannes Gutenberg-Universität Mainz, D-55099 Mainz, Germany

Received 10 April 2002; accepted 10 June 2002

Abstract

A progress report is given on the investigation of metal clusters with an ion cyclotron resonance (Penning) trap. The examples are taken from the recent studies on gold clusters. In particular, the monomer and dimer evaporation is monitored as a function of cluster size. For the particular case of Au_7^+ this study is expanded to include the energy dependence of the branching ratio. In connection with the sequential decay of Au_8^+ the information can be used for a model-free determination of the dissociation energy of Au_8^+. A second line of studies concerns the production, properties and storage behavior of polyanionic gold clusters. Such species have recently been produced by electron attachment to monoanionic gold clusters stored in the Penning trap. While collisional excitation may lead to ion loss due to changes of the ion motion upon electron emission, the competition between electron detachment and neutral atom evaporation can be studied by laser excitation. Small clusters tend to emit electrons, while larger ones evaporate atomic monomers. (Int J Mass Spectrom 219 (2002) 363–371)

Keywords: Penning trap; Ion cyclotron resonance; Metal cluster; Dissociation energy; Dianion

---

1. Introduction

The field of small inorganic clusters [1] has found widespread interest for quite a while (see e.g., the conference proceedings given in [2]), in particular after it was found in the early eighties that the properties of these particles do not show a smooth transition between single atoms or molecules and the bulk material. Instead, magic numbers were found, i.e., cluster sizes where the clusters have an increased stability as compared to the neighbor sizes [3,4]. These magic numbers are not universal but depend on the type of interaction between the clusters' constituents. There are two main groups: the properties may either be dominated by geometrical aspects, i.e., the spatial position of the atoms or molecules, or by the electronic structure, i.e., by the quantum mechanical level structure of delocalized valence electrons in a spherical or near spherical mean field potential. Prototype systems at the two extremes are the noble gas [3] and the alkali metal clusters [4]. However, usually the systems show a mixed behavior and the dominance of one aspect over the other may itself be a function of a cluster parameter as, e.g., the temperature or cluster size [5–7].

In order to study some of these aspects in further detail, a Penning ion trap apparatus has been setup [8–10] and applied to noble metal clusters. Ion trapping techniques allow one to obtain good control of the samples studied. In particular, the species of interest can easily be isolated, i.e., selected from a larger

---

[*] Corresponding author.
E-mail: lutz.schweikhard@physik.uni-greifswald.de

PII S1387-3806(02)00754-6

ensemble by ejection of all unwanted ions. This aspect is important with respect to the size selection of clusters, since in general cluster sources produce a wide distribution of cluster sizes and it can be difficult to disentangle their reactions without a prior size selection. In addition, the trap allows a cascading of selection and reaction. Thus, products of earlier reactions can be used for subsequent investigations, where the "product reactants" may not be available directly from a cluster source.

The second main advantage of ion trapping is the dynamic range with respect to time. The only alternative for the study of gas phase clusters is the cluster beam which limits the measurement duration to the flight time between the cluster source and the detector. The flight time of such a beam, however, is short compared to the trapping times which can be of the order of seconds in ion trapping devices. Such devices include the Penning trap which will be discussed in the following, similar other ICR systems, which make use of the Fourier transform-ion cyclotron resonance (FT-ICR) detection scheme [11–13], but also ion traps based on rf fields [14–18], electrostatic traps [19], and storage rings [20].

In the following, the recent progress of investigations at our Cluster Trap is reported. After a review of the setup two main lines of research are described for the case of gold clusters, the study of decay branching ratios and the production and study of polyanionic systems.

2. Experimental setup and procedure

A schematic overview of the experimental setup is given in Fig. 1. The components are described in detail elsewhere [8–10]. In a Smalley-type cluster ion source [21,22] singly-charged clusters are produced by laser vaporization of a metal wire in a helium gas pulse. The gas is expanded through a nozzle into differentially pumped vacuum sections and the clusters are guided by electrostatic ion-optical elements to the Penning trap where they are captured in flight [23] for extended storage. The trap consists of a homogeneous magnetic field of 5 T for radial and a quadrupolar electric field (potential well depths of a few volts) for axial ion confinement [24]. Several cluster ion bunches may be accumulated [25]. In the trap specific cluster sizes are selected by radial ion cyclotron resonance ejection of all unwanted ions. After this isolation step various interactions can be applied. The reactions are analyzed by axial ejection of the products and time-of-flight (TOF) mass spectrometry with single ion detection.

Fig. 2 shows a cartoon of a particular experimental event sequence, where anionic clusters are transferred/captured (a) and size-selected (b). After application of an electron beam and gas pulses the clusters pick up more electrons (c) and are again selected, now with respect to their charge state (d). With a laser beam the dianionic clusters can be transformed back to singly-charged species (e) and these final products

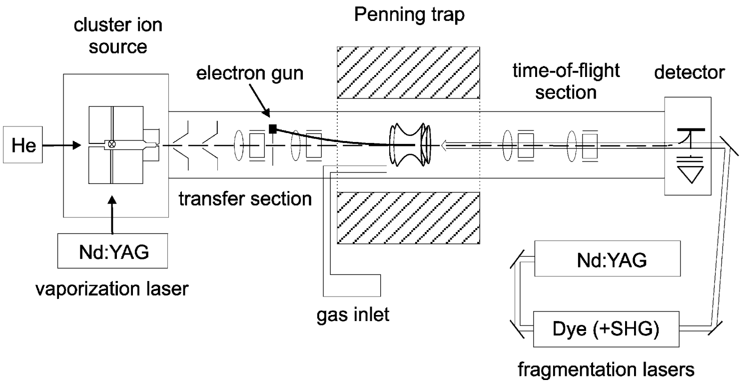

Fig. 1. Overview of the experimental setup.

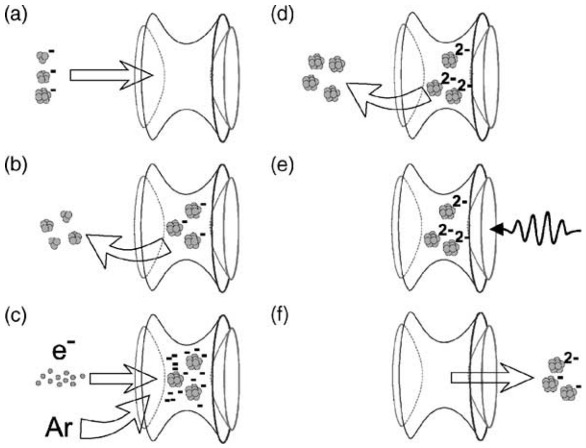

Fig. 2. Cartoon of the experimental event sequence for laser dissociation of stored cluster ions.

are detected by ejection into the TOF section (f). Further details of this particular experiment are given below (Section 4).

The sequence of Fig. 2 demonstrates how by use of several selection steps, it is possible to produce an ensemble with particular values of mass, *m*, and charge state, *z*, whereas in general mass spectrometric selection is only sensitive to the ratio *m*/*z*. Another example where this feature has been used is multiply charged positive metal clusters and in particular the case of $Ag_{16}{}^{2+}$ [26]. In order to find its fragmentation behavior and not to confuse it with the decay of $Ag_8{}^+$, the cluster has been produced indirectly: first, $Ag_{17}{}^{2+}$ has been formed by electron impact ionization of $Ag_{17}{}^+$. Collisional excitation of $Ag_{17}{}^{2+}$ leads to neutral monomer evaporation and thus $Ag_{16}{}^{2+}$ is generated without any $Ag_8{}^+$ present. After this step $Ag_{16}{}^{2+}$ can be selected with well defined size and charge state by ejection of the unwanted species and thus isolation of the desired *m*/*z*. Subsequent excitation of $Ag_{16}{}^{2+}$ leads to a fission into $Ag_{13}{}^+ + Ag_3{}^+$. Similarly, $Ag_{18}{}^{2+}$ has been prepared and observed to decay into $Ag_{15}{}^+ + Ag_3{}^+$, i.e., into two very different cluster sizes. Thus, in both cases much more symmetric fission reactions, as reported earlier [27], seem very unprobable in the light of the recent experiments [26].

3. Dimer vs. monomer evaporation of photoexcited clusters

Small singly-charged gold clusters, $Au_n{}^+$, evaporate either neutral monomers or dimers when excited above the dissociation threshold, as has been shown in detail [28,29]. As an example, Fig. 3 shows TOF spectra for the photodissociation of $Au_7{}^+$. After size selection (Fig. 3(a)) the clusters are irradiated with a laser pulse (at $\lambda = 355$ nm and a pulse energy of 30 μJ). The product yields for monomer and dimer evaporation, $Au_{n-1}{}^+$ and $Au_{n-2}{}^+$, are strongly dependent on the size of the precursor, $Au_n{}^+$, in particular on whether it consists of an even or odd number of atoms. Fig. 4 shows an overview of two series of measurements, where size-selected gold clusters have been irradiated with the 3rd (top) and 4th (bottom) harmonic of a Nd:YAG laser. The laser pulse energy has been limited to the range of single photon absorption. Thus, at the lower photon energy, for some clusters the excitation is not high enough for dissociation. Nevertheless, the odd–even effect in the decay pathway is clearly

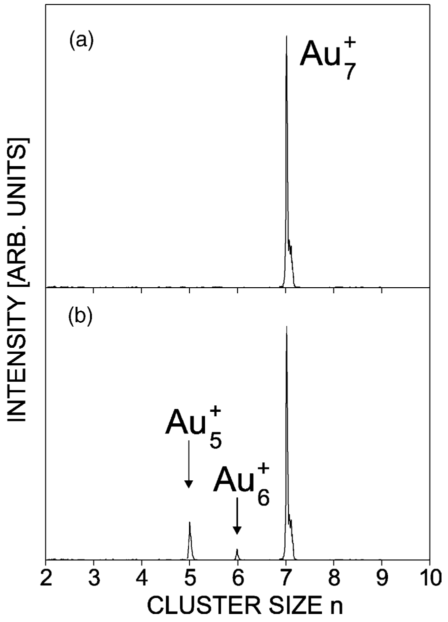

Fig. 3. TOF spectra of $Au_7{}^+$ (a) before and (b) after photoexcitation with a laser pulse of 30 μJ at $\lambda = 266$ nm.

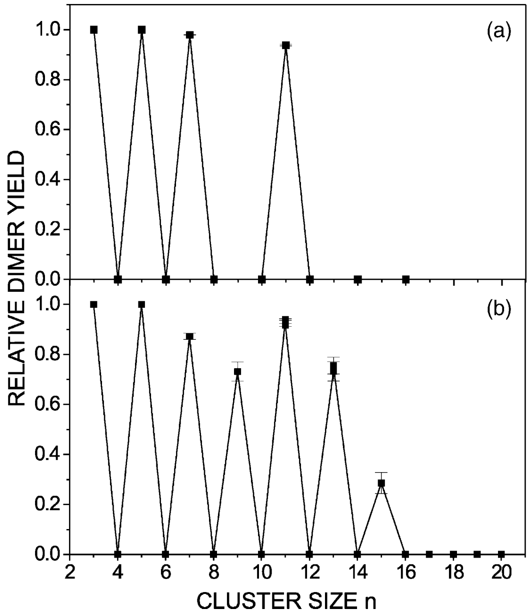

Fig. 4. Dimer vs. monomer evaporation yields of excited gold clusters as a function of clusters size for photoexcitation at (a) $\lambda = 355\,\mathrm{nm}$ and (b) $\lambda = 266\,\mathrm{nm}$.

visible. At the higher photon energy, all clusters can be dissociated and from these measurements it is evident that large clusters ($n \geq 16$) decay by monomer evaporation and the smaller ones show the odd–even effect.

A further examination of the relative yields shows that the branching ratio depends on the excitation energy, see for example, the values at $n = 7$. This feature can be used for the determination of dissociation energies with a recently developed procedure [30,31]. The idea and first application of the method was to avoid extensive modeling of rates and instead measure an extra set of rate constants. Specifically, the decay rate of a cluster $\mathrm{Au}_{n-1}{}^{+}$ was investigated for both the direct decay

$$\mathrm{Au}_{n-1}{}^{+} \rightarrow \mathrm{Au}_{n-2}{}^{+}$$

and the sequential decay

$$\mathrm{Au}_{n}{}^{+} \rightarrow \mathrm{Au}_{n-1}{}^{+} \rightarrow \mathrm{Au}_{n-2}{}^{+}$$

The excitation energies, E_{n-1} and E_n, respectively, of the two processes are adjusted so that the observed decay rates are the same for the direct decay and for the last process in the sequential decay. Then the difference $E_n - E_{n-1}$ equals the dissociation energy of $\mathrm{Au}_n{}^{+}$, plus the kinetic energy of the evaporated monomer, which is only a relatively small correction that can either be measured or calculated. Effectively, the dissociation rate of $\mathrm{Au}_{n-1}{}^{+}$ is used as an uncalibrated thermometer. It is therefore not necessary to model the dependence of the decay rate on energy or, equivalently, to model the “rest energy” of the cluster after its decay since it can simply be subtracted by use of the result of the direct decay measurement. The method is consequently as model-free as possible. It has recently been applied to the gold clusters $\mathrm{Au}_n{}^{+}$, $n = 14$–24 [30].

Soon after the new concept had been invented, it was realized that also experimental observables other than the rate constant could be used as a thermometer. As mentioned above, the branching ratio of the dissociation pathways may serve as such a variable. This has been checked for the dissociation energies of $\mathrm{Au}_{14}{}^{+}$ and $\mathrm{Au}_{16}{}^{+}$ for which values from both choices of thermometer are available. The comparison shows very good agreement between the rate and the pathway measurements [31]. This agreement allows an expansion of the range of application of this method to much smaller clusters sizes with confidence and it has been applied in order to determine the dissociation energy of $\mathrm{Au}_8{}^{+}$. Fig. 5 shows the pathway branching ratios f_2/f_1 of dimer vs. monomer evaporation of gold clusters $\mathrm{Au}_7{}^{+}$ as a function of photoexcitation energy for the direct decay of $\mathrm{Au}_7{}^{+}$ (data points on the left) and for the sequential decay after photoexcitation of $\mathrm{Au}_8{}^{+}$ (data point on the right).

The energy difference is determined by linear interpolation of the data points of the direct process and comparison with the result of the sequential process $\mathrm{Au}_8{}^{+} \rightarrow \mathrm{Au}_7{}^{+} \rightarrow \mathrm{Au}_{6/5}{}^{+}$ at a photoexcitation energy of 6.98 eV, i.e., for the absorption of two photons of the frequency-trippled Nd:YAG laser beam. The laser pulse energy of this measurement was kept as low as possible compatible with reasonable statistics (120 μJ) with a sequential decay yield (i.e., relative number of $\mathrm{Au}_{6/5}{}^{+}$ ions) of only 4% of all stored

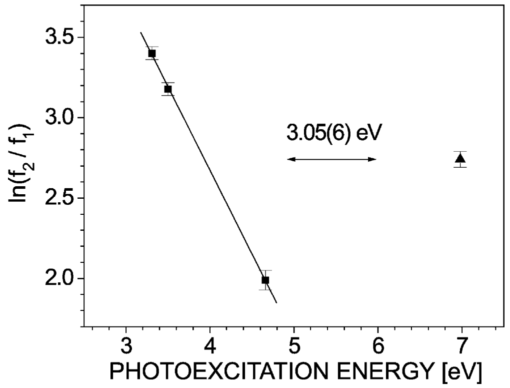

Fig. 5. Ratio of dimer (f_2) vs. monomer evaporation yields (f_1) of gold clusters $Au_7{}^+$ as a function of photoexcitation energy for the direct decay of $Au_7{}^+$ (data points on the left) and for the sequential decay after photoexcitation of $Au_8{}^+$ (data point on the right).

clusters. It was checked that the branching ratio does not depend on the laser pulse energy, which rules out any significant contribution from three or more photon absorption. The difference in photoexcitation energies for direct and sequential processes at a branching ratio f_2/f_1 (for dimer vs. monomer evaporation) of about 15 amounts to 3.05(6) eV. When the difference in initial thermal energies before photoexcitation (0.06 eV) and the kinetic energy of the evaporated monomer in the thermometer decay (0.46(5) eV) are taken into account (for details see [30,31]), the dissociation energy of $Au_8{}^+$ is determined to $D(Au_8{}^+) = 2.65(9)$ eV.

This number is of particular interest with respect to the investigations of the methanol gold cluster system $Au_n{}^+(CH_3OH)$: the time-resolved sequential and direct decays

$$Au_8{}^+(CH_3OH) \rightarrow Au_8{}^+ \rightarrow Au_7{}^+$$

$$Au_8{}^+ \rightarrow Au_7{}^+$$

are compared in order to study the binding of the methanol molecule to the gold cluster $Au_8{}^+$ [32]. Another area where a reliable value of the dissociation energy is of great interest, is the case of the vanadium cluster $V_{13}{}^+$. This cluster has been examined with respect to its radiative cooling behavior [33], but a comprehensive description had been difficult until the precise value of the dissociation energy was determined recently [34].

4. Production and study of dianionic gold clusters

While it is relatively easy to generate multiply positively charged metal clusters [35] and several investigations have been performed on such species with our Cluster Trap [36–39] the further charging of anionic ions to generate multiply negative systems is not as easy. However, it has been shown recently that additional electrons can be added if the cluster anions are bathed in a sea of electrons while both species are stored in an ICR trap [40–44]. In order to create such an electron bath argon gas pulses are applied to the trap region and an electron beam from an external source (located in the magnetic fringe field between the cluster source and the Penning trap) ionizes the argon atoms. In the negative axial trapping potential the cationic ions leave the trap immediately, but the secondary electrons that are formed in the ionization process remain stored in the trap—together with the anionic clusters that have been captured earlier in the sequence, as shown schematically in the cartoon of Fig. 2.

The procedure is also illustrated by the TOF spectra of $Au_{28}{}^-$ clusters as presented in Fig. 6, where the sequence has been interrupted by TOF analysis after size selection (a) and application of the electron bath (b). A number of studies have been performed with respect to the conversion yields from singly-charged cluster anions to higher charge states and these investigations show that the yield can be correlated with the magic numbers in the spherical shell model [41–43].

In a further step the dianionic clusters may be charge state selected (Fig. 6(c)). At this stage the dianionic clusters are available for further experiments. Recent experiments have shown that small clusters tend to emit one of the excess electrons upon excitation (Fig. 6(d)), whereas larger clusters cool by monomer evaporation (see below).

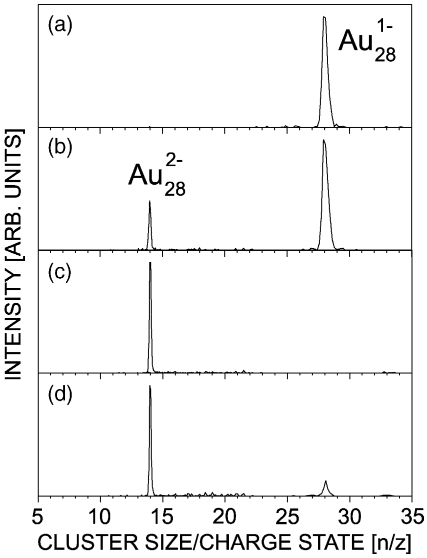

Fig. 6. TOF spectra of anionic gold clusters Au_{28} (a) after size selection ($Au_{28}{}^{-}$ only), (b) after application of an electron bath ($Au_{28}{}^{-}$ and $Au_{28}{}^{2-}$), (c) after charge state selection ($Au_{28}{}^{2-}$ only), and (d) after laser irradiation (wavelength $\lambda = 355$ nm, laser pulse energy 1 mJ, $Au_{28}{}^{-}$ and $Au_{28}{}^{2-}$).

With respect to ICR technology in general, it is of interest to investigate what happens to those clusters that lose an electron while they are on a large cyclotron radius, e.g., because the excitation has been imparted by collisions with gas molecules. Fig. 7 illustrates the radial motion in such a case. The top shows the pure cyclotron motion before the charge state changing electron emission. In the center diagram, the ion is assumed to lose the electron when it is at the indicated position (arrow). It continues with essentially the same speed $v = \omega_+\rho_+$. However, now the cyclotron frequency ω_+ has dropped by about a factor of 2 and in order to compensate this reduction the cyclotron radius ρ_+ has to increase by the same factor. At the same time the guiding center of the cyclotron revolution is shifted by ρ_+ away from the axis of the trap to produce a finite magnetron radius ρ_- equal to the initial cyclotron radius. Thus, the ion that moves on according to its new cyclotron and magnetron radii (Fig. 7(b) and (c)) now reaches out a factor 3 further away from the trap axis than before the reaction.

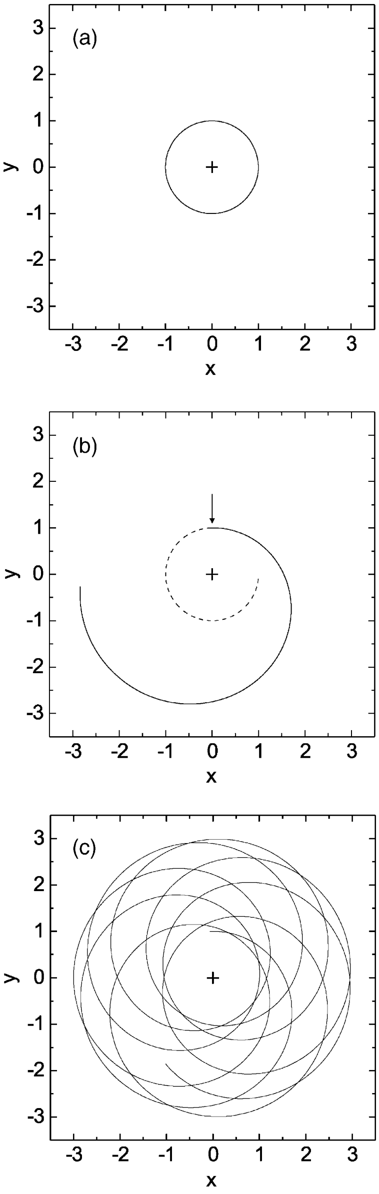

Fig. 7. Radial ion motion in the Penning trap illustrating the expansion of the ion motion's amplitude due to a sudden change in charge state: (a) cyclotron motion only, (b) change to a combination of cyclotron and magnetron motion when the charge state is reduced by a factor of 2, (c) resulting combined motion. (Axis in units of the initial cyclotron radius.)

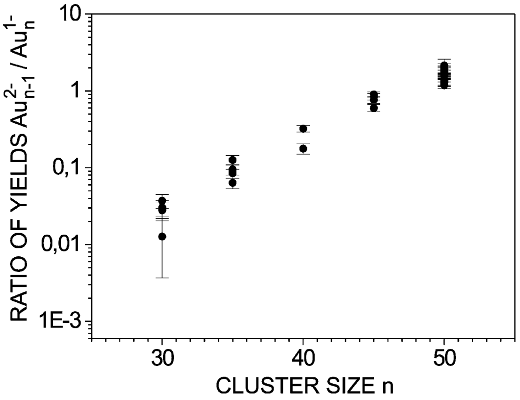

Fig. 8. Ratio of yields of dianionic products $Au_{n-1}{}^{2-}$ and singly-charged clusters $Au_n{}^-$ after photoexcitation (at $\lambda = 355$ nm) of size-selected dianionic gold clusters $Au_n{}^{2-}$ (preliminary results).

Since cluster ions are rather heavy species their center-of-mass collisional energy is relatively low and thus they have to be excited to rather large cyclotron radii to induce the electron emission. An increase of the ion orbits' radial extension by a factor 3, thus, often means the loss of the ion from the trap. Therefore, earlier experiments which used collisional excitation [45] have recently been extended and replaced by investigations via photoexcitation. Fig. 8 shows some preliminary results: the ratio of yields of reaction products due to neutral monomer evaporation

$$Au_n{}^{2-} \rightarrow Au_{n-1}{}^{2-} + Au$$

and due to electron emission

$$Au_n{}^{2-} \rightarrow Au_n{}^{-} + e^{-}$$

As described earlier [46] the droplet model of metal clusters [47] predicts a dissociation energy which does not change much as a function of cluster size. In contrast, the electron affinity of the anion, i.e., the excitation energy necessary for the emission of the second excess electron, is larger than the dissociation energy for large clusters but decreases as the cluster size is lowered. Thus, there is a transition region of cluster size below which the electron emission dominates over the dissociation. This predicted behavior is confirmed by the observation. Fig. 8 shows preliminary results of the ratio of yields of dianionic products $Au_{n-1}{}^{2-}$ and singly-charged clusters $Au_n{}^-$ after photoexcitation of size-selected dianionic gold clusters $Au_n{}^{2-}$. Within a cluster size region between $n = 30$ and 50 the decay pathway changes from more than 90% electron emission to dominantly neutral monomer decay. Note that as in the case of the monomer/dimer decay pathway competition described above, the branching ratio will, in general, be a function of the excitation energy. It may thus again be possible to use it for the investigation of dissociation energies and/or electron detachment energies.

5. Conclusion and outlook

Ion trapping has proven a versatile tool in the study of clusters, both because of the large range of time scales which can be investigated and because the trapping allows a number of manipulations to prepare the clusters with well defined excitation energies and well defined charge states which could not have been reached with the more common molecular beam techniques. In particular, the trap has been successfully applied to the measurement of binding energies. One result of these studies is that dissociation energies for medium size and small clusters can now be determined with an accuracy which allows detailed tests of statistical rate theories and provides a much needed absolute energy scale for competing processes such as radiative cooling and thermal electron emission. In addition, the application of an electron bath has led to the first observation of polyanionic metal clusters. These species are now available for further studies. The techniques described above may be combined for future even more detailed investigations of the transition from the isolated constituents of matter, i.e., atoms and molecules, to its condensed phase.

Acknowledgements

The reported investigations have been supported by the Deutsche Forschungsgemeinschaft, the Materials

Science Research Center Mainz, the European Union (the networks EUROTRAPS and CLUSTER COOLING) and the Fonds der Chemischen Industrie. A.H. and M.V. thank for stipends in the framework of the Graduiertenkolleg “Physik und Chemie supramolekularer Systeme.” K.H. acknowledges support by the Academy of Finland under the Finnish Center of Excellence Programme 2000–2005.

References

[1] H. Haberland (Ed.), Clusters of Atoms and Molecules, Springer, Berlin, 1994.

[2] Proceedings of the International Symposium on Small Particles and Inorganic Clusters (ISSPIC): Z. Phys. D 12 (1989) 1; Z. Phys. D 19 (1991) 1; Z. Phys. D 20 (1991) 1; Z. Phys. D 26 (1993) 1; Z. Phys. D 26 (1993) S1; Surf. Rev. Lett. 3 (1996) 1; Z. Phys. D 40 (1997) 1; Eur. Phys. J. D 9 (1999) 1; Eur. Phys. J. D 16 (2001) 1.

[3] O. Echt, K. Sattler, E. Recknagel, Phys. Rev. Lett. 47 (1981) 1121.

[4] W.D. Knight, K. Clemenger, W.A. de Heer, W.A. Saunders, M.Y. Chou, M.L. Cohen, Phys. Rev. Lett. 52 (1984) 2141.

[5] K. Rademann, B. Kaiser, U. Even, F. Hensel, Phys. Rev. Lett. 59 (1987) 2319.

[6] T.P. Martin, Phys. Rep. 273 (1996) 199.

[7] S. Krückeberg, G. Dietrich, K. Lützenkirchen, L. Schweikhard, C. Walther, J. Ziegler, Eur. Phys. J. D 9 (1999) 169.

[8] L. Schweikhard, S. Becker, K. Dasgupta, G. Dietrich, H.-J. Kluge, D. Kreisle, S. Krückeberg, S. Kuznetsov, M. Lindinger, K. Lützenkirchen, B. Obst, C. Walther, H. Weidele, J. Ziegler, Phys. Scripta T59 (1995) 236.

[9] L. Schweikhard, S. Krückeberg, K. Lützenkirchen, C. Walther, Eur. Phys. J. D 9 (1999) 15.

[10] L. Schweikhard, A. Herlert, M. Vogel, Metal clusters as investigated in a Penning trap, in: E.E.B. Campbell, M. Larsson (Eds.), Proceedings of the Nobel Symposium on the Physics and Chemistry of Clusters, Vol. 117, World Scientific, Singapore, 2001, p. 267.

[11] J.M. Alford, P.E. Williams, D.J. Trevor, R.E. Smalley, Int. J. Mass Spectrom. Ion Process. 72 (1986) 33.

[12] M.P. Irion, A. Selinger, R. Wendel, Int. J. Mass Spectrom. 96 (1990) 27.

[13] C. Berg, T. Schindler, G. Niedner-Schatteburg, V.E. Bondybey, J. Chem. Phys. 102 (1995) 4870.

[14] D.B. Cameron, J.H. Parks, Chem. Phys. Lett. 272 (1997) 18.

[15] D. Gerlich, Phys. Scripta T59 (1995) 256.

[16] S. Wolf, G. Sommerer, S. Rutz, E. Schreiber, T. Leisner, L. Wöste, Phys. Rev. Lett. 74 (1995) 4177.

[17] L. Wöste, Z. Phys. Chem. 196 (1996) 1.

[18] S. Krückeberg, D. Schooss, M. Maier-Borst, J.H. Parks, Phys. Rev. Lett. 85 (2000) 4494.

[19] A. Naaman, K.G. Bhushan, H.B. Pedersen, N. Altstein, O. Heber, M.L. Rappaport, R. Moalem, D. Zajfman, J. Chem. Phys. 113 (2000) 4662.

[20] P. Hvelplund, J.U. Andersen, K. Hansen, Clusters in storage rings, in: D.H.E. Dubin, D. Schneider (Eds.), AIP Conference Proceedings on Trapped Charged Particles and Fundamental Physics, Vol. 457, 1999, p. 220.

[21] D.E. Powers, S.H. Hansen, M.E. Geusig, A.C. Puiu, J.B. Hopkins, T.G. Dietz, M.A. Duncan, P.R.R. Langridge-Smith, R.E. Smalley, J. Phys. Chem. 86 (1982) 2556.

[22] H. Weidele, U. Frenzel, T. Leisner, D. Kreisle, Z. Phys. D 20 (1991) 411.

[23] H. Schnatz, G. Bollen, P. Dabkievicz, P. Egelhof, F. Kern, H. Kalinowsky, L. Schweikhard, H. Stolzenberg, H.-J. Kluge, Nucl. Inst. Meth. A 251 (1986) 17.

[24] L.S. Brown, G. Gabrielse, Rev. Mod. Phys. 58 (1986) 233.

[25] H.-U. Hasse, S. Becker, G. Dietrich, N. Klisch, H.-J. Kluge, M. Lindinger, K. Lützenkirchen, L. Schweikhard, J. Ziegler, Int. J. Mass Spectrom. Ion Process. 132 (1994) 181.

[26] S. Krückeberg, L. Schweikhard, G. Dietrich, K. Lützenkirchen, C. Walther, J. Ziegler, Chem. Phys. 262 (2000) 105.

[27] I. Katakuse, H. Ito, T. Ichihara, Int. J. Mass Spectrom. 97 (1990) 47.

[28] S. Becker, G. Dietrich, H.-U. Hasse, N. Klisch, H.-J. Kluge, D. Kreisle, S. Krückeberg, M. Lindinger, K. Lützenkirchen, L. Schweikhard, H. Weidele, J. Ziegler, Comp. Mater. Sci. 2 (1994) 633.

[29] M. Vogel, K. Hansen, A. Herlert, L. Schweikhard, Eur. Phys. J. D 16 (2001) 73.

[30] M. Vogel, K. Hansen, A. Herlert, L. Schweikhard, Phys. Rev. Lett. 87 (2001) 13401.

[31] M. Vogel, K. Hansen, A. Herlert, L. Schweikhard, Chem. Phys. Lett. 346 (2001) 117.

[32] M. Vogel, K. Hansen, A. Herlert, L. Schweikhard, C. Walther, J. Chem. Phys. 116 (2002) 9658.

[33] C. Walther, G. Dietrich, W. Dostal, K. Hansen, S. Krückeberg, K. Lützenkirchen, L. Schweikhard, Phys. Rev. Lett. 83 (1999) 3816.

[34] C. Walther, K. Hansen, A. Herlert, S. Krückeberg, K. Lützenkirchen, L. Schweikhard, M. Vogel, Phys. Rev. A, in preparation.

[35] U. Näher, S. Bjørnholm, S. Frauendorf, F. Garcias, C. Guet, Phys. Rep. 285 (1997) 245.

[36] L. Schweikhard, P. Beiersdorfer, W. Bell, G. Dietrich, S. Krückeberg, K. Lützenkirchen, B. Obst, J. Ziegler, Hyp. Interact. 99 (1996) 97.

[37] S. Krückeberg, G. Dietrich, K. Lützenkirchen, L. Schweikhard, J. Ziegler, Phys. Rev. A 60 (1999) 1251.

[38] J. Ziegler, G. Dietrich, S. Krückeberg, K. Lützenkirchen, L. Schweikhard, C. Walther, Int. J. Mass Spectrom. 202 (2000) 47.

[39] S. Krückeberg, G. Dietrich, K. Lützenkirchen, L. Schweikhard, C. Walther, J. Ziegler, J. Chem. Phys. 114 (2001) 2955.

[40] A. Herlert, S. Krückeberg, L. Schweikhard, M. Vogel, C. Walther, Phys. Scripta T80 (1999) 200.

[41] L. Schweikhard, A. Herlert, S. Krückeberg, M. Vogel, C. Walther, Philos. Mag. B 79 (1999) 1343.

[42] A. Herlert, L. Schweikhard, M. Vogel, Eur. Phys. J. D 16 (2001) 65.
[43] C. Yannouleas, U. Landman, A. Herlert, L. Schweikhard, Phys. Rev. Lett. 86 (2001) 2996.
[44] A. Herlert, R. Jertz, J. Alonso Otamendi, A.J. González Martínez, L. Schweikhard, Int. J. Mass Spectrom. 218 (2002) 217.
[45] A. Herlert, L. Schweikhard, M. Vogel, Charge-changing reactions and their influence on the ion motion in a Penning trap, in: F. Anderegg, L. Schweikhard, C.F. Driscoll (Eds.), AIP Conference Proceedings on Non-Neutral Plasma Physics IV, Vol. 606, 2002, p. 652.
[46] C. Stoermer, J. Friedrich, M.M. Kappes, Int. J. Mass Spectrom. 206 (2001) 63.
[47] S. Bjørnholm, Shell structure in atoms, nuclei and in metal clusters, in: H. Haberland (Ed.), Clusters of Atoms and Molecules, Springer, Berlin, 1994.